Solidly Mounted Resonators with Carbon Nanotube Electrodes for Biosensing Applications

García-Gancedo L.[1], Iborra E.[2], Clement M.[2], Olivares J.[2], Zhu, Z.[1], Flewitt A.J.[1], Milne W.I.[1], Ashley G.M.[3], Luo J.K.[3], Zhao X.B.[4] and Lu J.R.[4]

[1] Electrical Engineering Division, University of Cambridge, Cambridge, United Kingdom
[2] Grupo de Microsistemas y Materiales Electrónicos, Universidad Politécnica de Madrid, Madrid, Spain
[3] IMRI, University of Bolton, Bolton, United Kingdom
[4] School of Physics & Astronomy, University of Manchester, Manchester, United Kingdom

***Abstract*— The work reported here shows a direct experimental comparison of the sensitivities of AlN solidly mounted resonators (SMR)-based biosensors fabricated with standard metal electrodes and with carbon nanotube electrodes. SMRs resonating at frequencies around 1.75 GHz have been fabricated, some devices using a thin film of multi-wall carbon nanotubes (CNTs) as the top electrode material and some identical devices using a chromium/gold electrode. Protein solutions with different concentrations were loaded on the top of the resonators and their responses to mass-load from physically adsorbed coatings were investigated. Results show that resonators using CNTs as the top electrode material exhibited higher frequency change for a given load due to the higher active surface area of a thin film of interconnecting CNTs compared to that of a metal thin film electrode and hence exhibited greater mass loading sensitivity. It is therefore concluded that the use of CNT electrodes on resonators for their use as gravimetric biosensors is viable and worthwhile.**

I. INTRODUCTION

Gravimetric sensing is a well known technique utilised to detect the variation in a measurable parameter as a function of the deposited mass on an active sensing area [1-3]. Quartz crystal microbalances (QCM) resonating in the range of 5-20 MHz are one of the earliest, most successful examples of gravimetric sensors. Historically, the emergence of the Quartz crystal as a microbalance can be traced back to Sauerbrey, who realised that a resonating quartz crystal could be used for the microgravimetric measurement of sputtered thin films [4]. A few years later, King chemically sensitised a QCM to make selective chemical mass measurements of 10^{-9}g [5]. Since then, there has been an increased interest in developing gravimetric sensors with higher sensitivities for their use as biosensors. Mass loading sensitivity is proportional to the square of the operating frequency [4]; hence the emergence of bulk acoustic wave resonator (BAW) technology, a nanoscale version QCM with an operating frequency in the range of a few GHz, offered great potential to improve the sensitivity and detection limitation of gravimetric sensors. BAW resonators offer the additional advantage of lower fabrication cost due to the employment of microfabrication technologies and small dimensions, which makes them suitable for the fabrication of array of sensors for parallel or multi detection.

However, higher frequency and smaller dimensions cause all environmental and boundary conditions to affect the operation of the BAW resonators more strongly than the QCMs, resulting in a higher noise level and lower quality factors. It is for this reason that up to now, mass sensitivity of BAW resonators is not significantly better than that of QCMs [6-8].

Work has been carried out in the last few years towards the improvement of the structural and electrical properties of piezoelectric thin films for their use as the active material in these devices [9-12], with the aim of improving the electrical response of the resonators through the achievement of materials with improved piezoelectric properties. Recently, it has also been understood that the electrode material also plays an important role in the resonator's electrical response [13-16]. Electrodes not only affect the growth of the piezoelectric thin film but also provide the shape of the resonant area and, if designed properly, can confine the acoustic energy between the facets of the resonator thereby minimising losses and maximising electro-mechanical transduction (hence *Q*). Ideally, the electrode material should have low mass (in order to minimise mass-loading effects) but high acoustic impedance (in order to confine the acoustic waves within the piezoelectric layer) and high conductivity (in order to minimising the series resistance in the transmission of the excitation signal). Aluminium (Al), molybdenum (Mo)

The work reported here was supported by the EPSRC, grants number EP/F063865/1, EP/F06294X/1, EP/F062966/1 and EP/E023614/1. Iborra, Clemet and Olivares acknowledge financial support from the Ministerio de Ciencia e Innovación of Spain through project MAT2010-18933, and from the European Union through the European Regional Development Fund (FEDER).

tungsten (W), gold (Au) and platinum (Pt) are the most common metals utilised as the electrode materials. However the low acoustic impedance of Al and high weight of Mo, W, Au and Pt make them less ideal for their use as the electrode materials.

Carbon nanotubes (CNTs) have been shown to be an excellent material choice for BAW resonators [15-16]. They possess low densities in the range of 1-2 g·cm^{-3}, electrical conductivities of up to 10^6 S·m^{-1} and exceptionally high elastic moduli (hence high acoustic impedance), usually higher than 1 TPa [17]. Fig. 1 shows a comparison of densities and acoustic impedances of some of the commonly used metals for electrodes, and highlights that CNTs posses the highest acoustic impedance and lowest density allowing simultaneously low mass electrodes with high acoustic impedance and low series resistance.

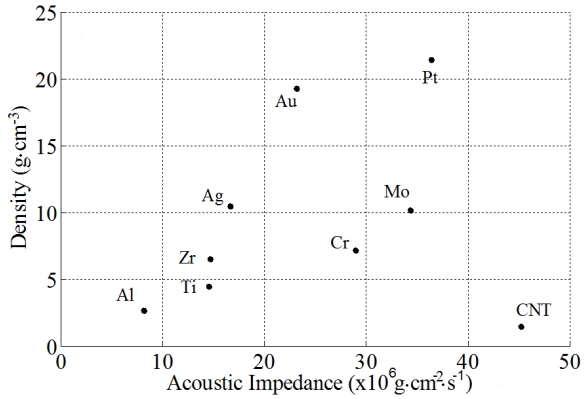

Figure 1. Density and acoustic impedance of commonly used electrode metals

Biosensors with CNT electrodes will offer an additional benefit compared to those with metal electrodes as it is possible to post-growth functionalise them for direct bonding to targeted molecules, thereby preventing non-specific binding or the need of additional bonding layers. Hence the potential exists to use chemically modified CNTs which would double both as the electrode and the sensing layer. Recent advances in chemical functionalisation of CNTs in sensing systems have been reported in [18-23]. Furthermore, the surface area of a thin film of interconnecting CNTs is significantly higher than the surface area of a metal thin film electrode; hence the binding area is increased without physically increasing the size of the devices. Consequently, for the same concentration of biological samples, a greater number of targeted molecules can be bound onto the resonator's surface compared to devices with metal electrodes, and hence devices with higher sensitivity can be realised.

The work reported here shows a direct experimental comparison of the sensitivity of AlN SMRs biosensors with standard metal electrodes and with CNT electrodes. SMRs resonating at frequencies around 1.75 GHz have been fabricated, some devices using a thin film of multi-wall CNTs as the top electrode material, and some identical devices using a top chromium/gold electrode. The CNTs were directly grown on the AlN film from an iron seed layer at 650°C in a NH_3 and C_2H_2 atmosphere, and possess very low density (<2 g cm^{-3}), high electrical conductivities (>10^5 S/m), and exhibited excellent definition and adhesion to the surface. Bovine Serum Albumin (BSA) solutions with different concentrations were loaded on the top of the resonators and their responses to mass-load from physically adsorbed protein coatings were investigated.

II. Experimental Methods

A. AlN SMR fabrication

SMRs were fabricated by growing Ir/AlN/CNT stacks on top of acoustic mirrors centred at a frequency of around 2 GHz and formed by five alternating low and high acoustic impedance layers of porous SiO_2, with an acoustic impedance of 9.5×10^6 kg·m^{-2}·s^{-1} [24], and Ir, with an acoustic impedance of 138.0×10^6 kg·m^{-2}·s^{-1} [25]. A seed layer of Ti/Mo (15-20 nm thick) was used to improve the adhesion and crystal quality of the Ir bottom electrode to the acoustic reflector. Ir slugs (99.98% pure) were electron-beam evaporated at a base pressure of less than 1×10^{-6} Torr to form bottom electrodes 120 nm thick. The AlN piezoelectric films were then reactively sputtered from a 150 mm in diameter Al target in a Leybold Z-550 sputtering system. Before AlN deposition, a 60 s soft-etch in an Ar discharge was performed to condition the Ir bottom electrode. AlN films were sputtered with a 3:7 Ar/N_2 admixture at a total pressure of 1.2 mTorr, a pulsed DC power level of 1.2 kW, and a substrate temperature of 400º C. An RF bias was applied to the substrates to tune the stress in the AlN films and to improve their crystal structure and orientation. These conditions yielded a deposition rate of 40 nm·min^{-1}. The thickness of the AlN layer was set to 1550 nm.

The crystal structure of the AlN and Ir films was assessed by X-ray diffraction (XRD) through the measurement of the θ/2θ patterns and the rocking-curves (RC) around the most intense reflections, i.e. the AlN 00·2 at 18.02º (θ) and the Ir (111) at 20.35º (θ). The surface of the different layers was inspected by atomic force microscopy (AFM), which provided the measurement of the surface roughness. Additional information on the polar orientation was obtained by wet chemical etching of the AlN layers.

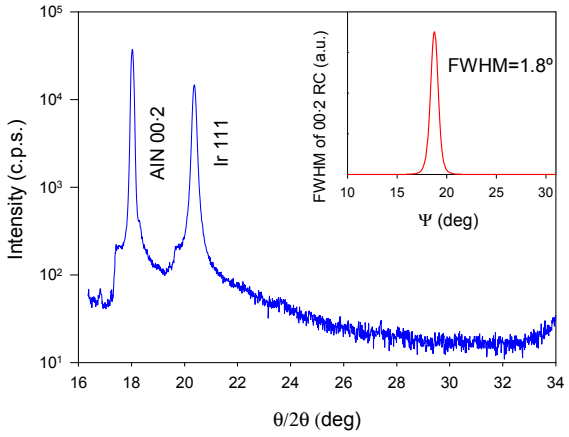

Figure 2. XRD patterns of AlN on Ir. The inset show the rocking curve (RC) of the 00·2 AlN peak.

XRD characterisation showed that highly *c*-axis-oriented AlN films were successfully grown on (111)-oriented Ir layers, provided these surfaces were etched with Ar+ ions immediately before AlN deposition (see Fig. 2). The pre-treatment of the Ir surface was essential to avoid the growth of tilted microcrystals related to the degradation of the piezoelectric response; AlN films with pure 00·2 orientation and RC ranging from 1.8º to 3º, almost independent of the texture and roughness of the Ir bottom electrode, were obtained. No degradation of the piezoelectric quality of AlN films with the texture was observed in the mentioned range.

Fig. 3 shows atomic force microscopy (AFM) images of the surface of Ir electrode (before AlN deposition) and AlN films. The roughness of the Ir electrode is around 4 nm and that of AlN films is around 7 nm. The structure of the AlN surface indicates a *c*-axis orientation of the microcrystals with a basal plane diameter of around 50 nm.

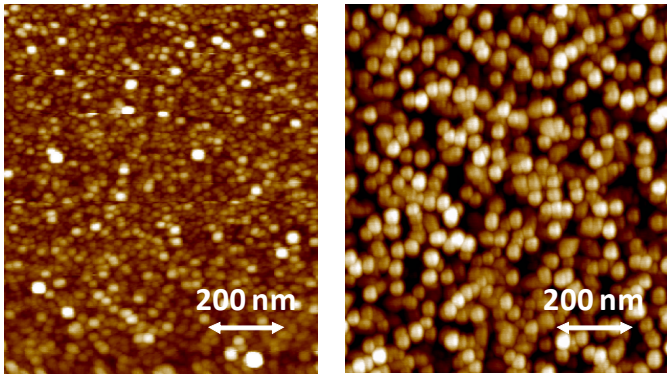

(a) (b)

Figure 3. AFM images of the surfaces of : (a) Ir bottom electrode before AlN deposition and (b) AlN film.

After AlN deposition, vias were formed through the AlN for electrical connection to the bottom electrode by wet etching the AlN in a warm (40°C) KOH solution through a Mo mask. The top electrode was then patterned with a lift-off photolithography process. At this point, a 10 nm of Cr layer followed by a 90 nm of Au layer was evaporated on one set of devices. A 7 nm of Fe layer, which acts as a catalyst layer for the CNTs growth, was evaporated on another set of devices. The CNTs were directly grown on the second set of the devices, as explained in the following section.

Fig. 4 shows the top view of one of the devices fabricated with top CNTs electrode. It can be seen that the definition of the electrodes is excellent.

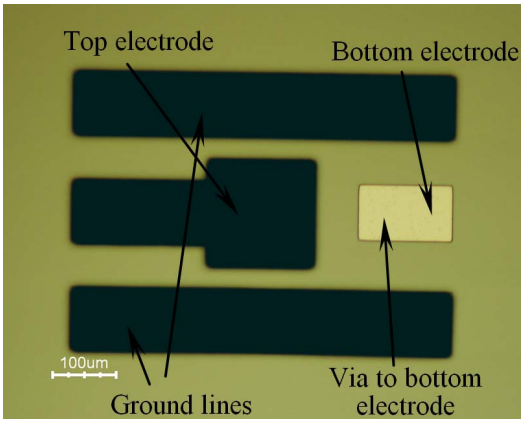

Figure 4. Image of a fabricated SMR with CNT top electrode

B. *CNT growth and characterisation*

CNT growth was carried out by thermal CVD. The substrate was loaded into the chamber and heated up to 650 °C at a rate of 4°C/min. Ammonia (NH_3) was introduced into the chamber to raise the pressure up to 5 mbar. It also helped to maintain the catalyst metal surface activity by reacting with the amorphous carbon. The system was maintained for several minutes so as to break the catalyst layer into nanoislands, after which acetylene (C_2H_2) was introduced into the chamber to commence the growth. C_2H_2 is the source of carbon necessary for CNT growth, and was introduced into the chamber through a large, flat, stainless steel plate 'showerhead' configuration, which ensures a uniform flow of gas over the whole area of growth. Once the growth is finished, the gases were evacuated and the system was left to cool down. This type of growth produces a forest of interconnecting nanotubes that should possess optimal electromechanical properties [17]. However if no particular care is taken, CVD generally produces CNTs with numerous defects. A high density of defects are favoured when the growth occurs at low temperatures, dopants such as N_2 or B are present or a residual growth process continues when the power is shutdown, but the gases are not turned off.

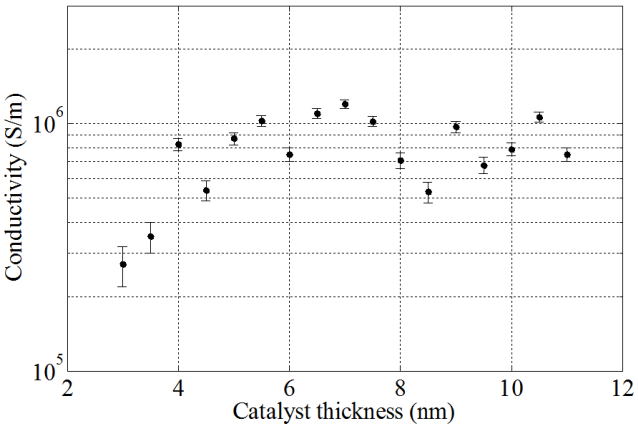

Figure 5. Conductivity of the CNTs layer *vs*. catalyst layer thickness for growth temperature of 750 ºC

The gas ratio C_2H_2 / NH_3 and growth temperature were optimised so as to avoid the presence of amorphous carbon, which would decrease significantly the conductivity. The catalyst layer thickness was varied in order to clarify its effect on the conductivity of the CNT layer. It was found that the conductivity increases with the catalyst thickness up to ~5nm, and become less thickness dependent afterwards as shown in Fig. 5.

The growth temperature was also changed in order to maximise the conductivity. A higher growth temperature produces CNT layers with a higher conductivity, as shown in Fig. 6, due to lower number of defects. However when growing the CNTs on top of an acoustic mirror, the Ir layers on the reflector stack delaminate, damaging a large number of devices. For this reason, when the growth temperature is 750 ºC, the yield is only around ~10%. Lowering the growth temperature to 650 ºC decreases slightly the conductivity but increases the yield to around ~20%. Growth does not occur at temperatures below ~600 ºC under these experimental conditions.

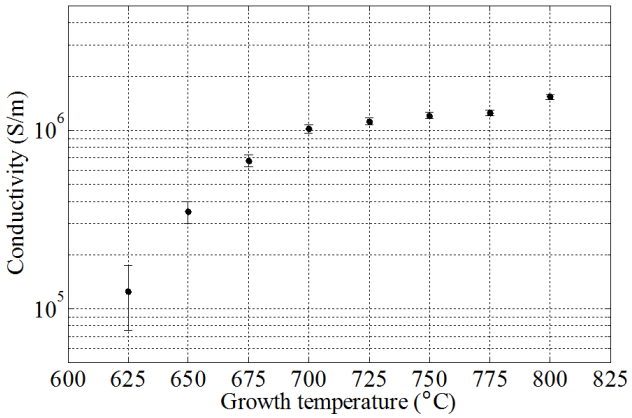

Figure 6. Conductivity of the CNTs layer vs. growth temperature

In this work CNTs were grown at 650 ºC with a catalyst thickness of 7 nm. CNT layers obtained possess an electrical conductivity of ~3.5×10^5 S/m.

III. FBAR Electrical Characterisation

Electrical characterisation of the SMR devices was carried out using an Agilent E5061B network analyser. An automation measurement routine was written with LabView to continuously monitor and record the resonance spectrum of the SMRs. Devices resonating at around 1.75 GHz, with resonance spectra that were free from significant spurious modes, were achieved and a typical response of the devices with CNT electrodes is shown in Fig. 7. It was also found that the resonant frequency of the devices covered with CNT electrodes is slightly higher due to the lower mass of the CNT electrodes compared to the Cr/Au electrodes.

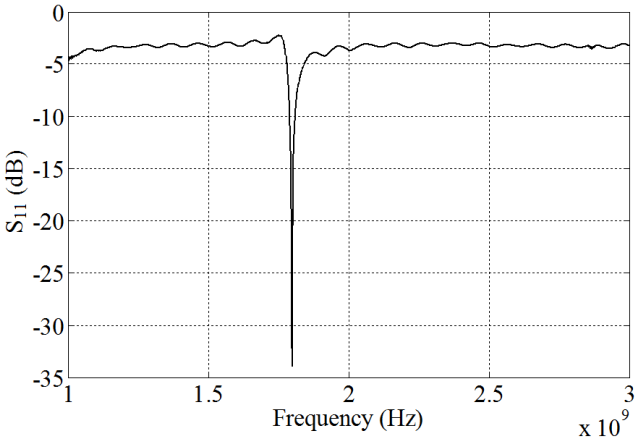

Figure 7. Typical frequency response of fabricated devices with CNT top electrode, showing the main resonance at f_0 ~ 1.75 GHz.

The quality factor of the resonance peak was calculated using the 3-dB method [26] from the equation:

$$Q_{3dB} = \frac{f_r}{|f_2 - f_1|} \tag{3}$$

where f_r is the resonant frequency taken from the S-parameter and f_1 and f_2 are the frequencies at which the insertion/return loss are +3 dB compared to the insertion/return loss at f_r.

Q was found to be higher than 2000 for the devices with CNT electrodes and around 1000 for the devices with metal electrodes. Generally devices with higher Q exhibit sharper resonance peaks that allow tracking a smaller frequency shift. Therefore, CNT electrode BAW resonators have the potential to measure smaller frequency shifts, increasing the sensitivity compared to the metal electrode devices.

IV. Preparation of Bio Targets on Devices and Biosensing Results

The resonant frequency of unloaded resonators was tracked over 30 min and was found to be stable with changes of less than 2 kHz. Bovine Serum Albumin (BSA) solutions with different concentrations (62.5, 125, 250, 500 and 1000 µg/ml) were then placed on the top of different sets of identical SMRs both with metals and CNT electrodes, and allowed them to physically adsorb onto the SMRs' surface for 15 min, after which they were rinsed by buffer and dried with N_2. Measurements were subsequently carried out on loaded devices when they are completely dried to monitor the frequency shift (compared to unloaded devices), and results are shown in Fig. 8 as a function of BSA concentration. The frequency shift was of the order of hundreds of kHz, and has a distinct linear relation with the solution concentration over the range measured. The absolute frequency changes observed on the SMRs with CNT electrodes are significantly greater than

those with metal electrodes, demonstrating its high performance and great potential for use.

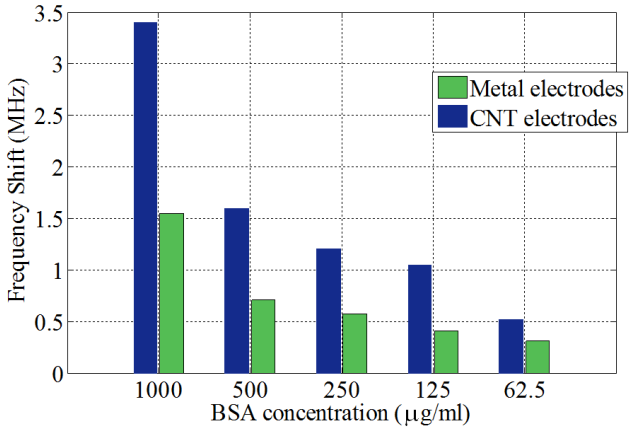

Figure 8. Frequency shift observed as a function of protein concentrations

V. CONCLUSIONS

BAW resonators with CNT electrodes have been shown to have many advantages for the development of acoustic wave based biosensors. AlN SMRs with a top CNT electrode resonating at around 1.75 GHz were microfabricated and exhibited a significantly large unloaded quality factor Q>2000, much greater than the identical devices fabricated with metal electrodes, which is a direct consequence of the low density and high acoustic impedance of the CNT electrodes. Devices with higher *Q* possess higher sensitivity due to sharper resonance peaks which facilitates tracking smaller frequency shifts. Furthermore, protein solutions with different concentrations were loaded on the top of the resonators and their responses to mass-load from physically adsorbed coatings were investigated. It was found that resonators using CNTs as the electrode material exhibited higher frequency change for a given load due to the higher surface area of a thin film of interconnecting CNTs compared to that of a metal thin film electrode.

VI. REFERENCES

[1] S.W. Wenzel and R.M. White, "*Analytic comparison of the sensitivities of bulk-wave, surface-wave and flexural plate-wave ultrasonic gravimetric sensors,*" Appl. Phys. Lett. Vol. 54 (20), pp. 1976-1978, 1989

[2] D.S. Ballantine, R.M. White *et al*., "*Acoustic wave sensors: theory, design and physico-chemical applications,*" R. Stern, M. Levy (Eds.), Applications of Modern Acoustics, Academic Press, San Diego, 1997

[3] M.D. Ward, D.A. Buttry *et al*., "*In situ interfacial mass detection with piezoelectric transducers*," Science, Vol. 249 1000–1007, 1990

[4] G. Sauerbrey, "*Erwendung von schwingqarzen zur wagung dunner schichten un zur mikrowagung*," Z. Physik, Vol. 155, pp. 206-222, 1959

[5] W.H. Jr. King, "*Piezoelectric sorption detector*," Anal. Chem. Vol. 36 (9), pp. 1735-1739, 1964

[6] J. Weber, W.M. Albers *et al*., "*Shear mode FBARs as highly sensitive liquid biosensors*," Sens. & Actuat. A: Phys., Vol. 128 (1), pp. 84-88, 2006

[7] G. Wingqvist, J. Bjurstrom *et al*., "*Immunosensor utilizing a shear mode thin film bulk acoustic sensor*," Sens. & Act. B: Chem., Vol. 123 (1), pp. 466-473, 2007

[8] G. Wingqvist, V. Yantchev *et al*., "*Shear mode AlN thin film electro-acoustic resonant sensor operation in viscous media*," Sens. & Act. A: Phys., vol. 148 (1), pp. 88-95, 2007

[9] P.B. Kirby, M.D.G. Potter *et al*., "*Thin film piezoelectric property considerations for surface acoustic wave and thin film bulk acoustic resonators*," J. Eur. Ceram. Soc., Vol. 23, pp. 2689-2692, 2003

[10] E. Iborra, M. Clement *et al*., "*Optimization of thin AlN sputtered films for X-band BAW resonators*," IEEE Ultrason. Symp. In press, 2010

[11] G. Ferblantier, F. Mailly *et al*., "*Deposition of zinc oxide thin films for application in bulk acoustic wave resonator*," Sens. & Act A, Vol. 122, pp. 184-188, 2005

[12] S-H. Choi and J-S Kim, "*Study on the c-axis preferred orientation of ZnO film on various metal electrodes*," Ultramiscroscopy, Vol. 108, pp. 1288-1291, 2008

[13] T. Yokoyama, T. Nishihara *et al.*, "*New electrode material for low-loss and high Q FBAR filters*," IEEE Ultrason. Symp., pp. 429-432, 2004

[14] S. Tanifuji, Y. Aota et al., "*Spurious vobration suppression by film thickness control FBAR*" IEEE Ultrason. Symp., pp. 2193-2196, 2008

[15] M. Dragoman, A. Muller et al., "*High performance thin film bulk acoustic resonator covered with carbon nanotubes*," App. Phys. Lett., Vol. 89, 143122, 2006

[16] L. Garcia-Gancedo, F. Al-Naimi *et al*., "*Fabrication of High-Q Film Bulk Acoustic Resonator (FBAR) Filters with Carbon Nanotube (CNT) electrodes*", IEEE Ultrason. Symp. 2010

[17] M. Mann, Y. Zhang *et al*., "*Controlling the growth of carbon nanotubes for electronic devices*," Microelectronic Engineering, Vol. 87 (5-8), pp. 1491-1493, 2010

[18] S. Liu, Q. Shen *et al.*, "*Chemical functionalization of single-walled carbon nanotube field-effect transistors as switches and sensors*," Coord. Chem. Revs., Vol. 254, pp. 1101-1116, 2010

[19] A. Star, J.P Gabriel *et al*. "*Electronic detection of specific protein binding using nanotube FET devices*," Nanoletters, Vol. 3, pp. 459-463, 2003.

[20] P. Qi, O. Vermesh *et al*., "*Toward large arrays of multiplex functionalized carbon nanotube sensors for highly sensitive and selective molecular detection*," Nanoletters, Vol. 3, pp. 347-351, 2003.

[21] J.F. Lu, L. Gu *et al*., "*Advances in bioapplications of carbon nanotubes*," Advanced Mat., Vol. 21, pp. 139-151, 2009.

[22] A. Modi, N. Koratkar *et al*., "*Miniaturized gas ionization sensors using carbon nanotubes*," Nature, Vol. 424, pp. 171-174, 2003.

[23] J. Li, A.M. Cassell *et al*., "*Carbon nanotubes as AFM tips: Measuring DNA molecules at the liquid/solid interface*," Surf. & Interf. Anal., Vol. 28, pp. 8-11, 1999

[24] A. Devos, E. Iborra *et al*., "*Picosecond ultrasonics as a helpful technique for introducing a new electrode material in BAW technology: the iridium case*," IEEE Ultrason. Symp., pp. 1433-1436, 2007.

[25] J. Olivares, E. Wegmann *et al*., "*Sputtered SiO_2 as low acoustic impedance material for bragg mirror fabrication in BAW resonators*", IEEE Trans. Ultrason. Ferr. Freq. Control., in press.

[26] K. J. Coakley, J. D. Splett *et al*., "*Estimation of Q factors and resonant frequencies*," IEEE Trans. Micro. Theo. & Tech., Vol. 51, pp. 862 – 868, 2003